Drug Repurposing Using Molecular Network Analysis Identifies Jak as Targetable Driver in Necrobiosis Lipoidica

Alysia N. Hughes[1], Xing Li[1], Julia S. Lehman[2,3], Steven A. Nelson[1], David J. DiCaudo[1], Rekha Mudappathi[4,5,6], Angelina Hwang[1], Jacob Kechter[1], Mark R. Pittelkow[1], Aaron R. Mangold[1] and Aleksandar Sekulic[7,8]

Drug repurposing is an attractive strategy for therapy development, particularly in rare diseases where traditional drug development approaches may be challenging owing to high cost and small numbers of patients. In this study, we used a drug identification and repurposing pipeline to identify candidate targetable drivers of disease and corresponding therapies through application of causal reasoning using a combination of open-access resources and transcriptomics data. We optimized our approach on psoriasis as a disease model, demonstrating the ability to identify known and, to date, unrecognized molecular drivers of psoriasis and link them to current and emerging therapies. Application of our approach to a cohort of tissue samples of necrobiosis lipoidica (an unrelated; rare; and, to date, molecularly poorly characterized cutaneous inflammatory disorder) identified a unique set of upstream regulators, particularly highlighting the role of IFNG and the Jak−signal transducer and activator of transcription pathway as a likely driver of disease pathogenesis and linked it to Jak inhibitors as potential therapy. Analysis of an independent cohort of necrobiosis lipoidica samples validated these findings, with the overall agreement of drug-matched upstream regulators above 96%. These data highlight the utility of our approach in rare diseases and offer an opportunity for drug discovery in other rare diseases in dermatology and beyond.

Keywords: Bioinformatics, Drug development, Gene Regulation, Genomics, Inflammatory, Skin diseases

JID Innovations (2024);**4:**100296 doi:10.1016/j.xjidi.2024.100296

INTRODUCTION

New drug development generally takes 10−15 years and costs >$2 billion (Pushpakom et al, 2019). Only 10% of drugs that successfully complete phase 1 clinical trial are approved by the United States Food and Drug Administration (FDA) (Dowden and Munro, 2019). Repurposing of existing drugs can reduce the time, risk, and cost associated with drug development, offering a more efficient and effective alternative to traditional approaches (Fetro and Scherman, 2020; Paik et al, 2015; Pushpakom et al, 2019; Roessler et al, 2021; Sirota et al, 2011; Weth et al, 2024; Zador et al, 2018).

Drug repurposing is particularly attractive for rare diseases where the study of disease mechanisms and development of potential therapies are challenging. Although individually, rare diseases (defined as affecting <200,000 people in the United States) affect a small percentage of the population, it is estimated that collectively, they affect 300 million people worldwide or 30 million people in the United States, translating to 1 in 10 in the United States, on par with the prevalence of type 2 diabetes (Marwaha et al, 2022) (https://www.orpha.net/consor/cgi-bin/index.php), highlighting the need for innovative drug discovery approaches.

Changes in gene expression patterns have been studied in many disease states. However, identifying the root cause leading to altered gene expression patterns and associated disease phenotype remains challenging (Bradley and Barrett, 2017). Several groups have tackled this challenge, deploying approaches ranging from the use of Toxicology Genomics Database, which collates experimental data of exposures to chemicals, drugs, and toxicants (Nguyen et al, 2023), to approaches using elegant animal models to identify gene expression changes in model disease states, validating such changes in human samples, and performing a focused candidate analysis for drug targeting (Srivastava et al, 2018). However, requirement for cell and animal models to generate

[1]*Department of Dermatology, Mayo Clinic, Scottsdale, Arizona, USA;* [2]*Department of Dermatology, Mayo Clinic, Rochester, Minnesota, USA;* [3]*Department of Laboratory Medicine and Pathology, Mayo Clinic, Rochester, Minnesota, USA;* [4]*Department of Quantitative Health Sciences, Mayo Clinic, Scottsdale, Arizona, USA;* [5]*Center for Individualized Medicine, Mayo Clinic, Scottsdale, Arizona, USA;* [6]*College of Health Solutions, Arizona State University, Phoenix, Arizona, USA;* [7]*Integrated Cancer Genomics Division, Translational Genomics Research Institute, Phoenix, Arizona, USA; and* [8]*City of Hope, Phoenix, Arizona, USA*

Correspondence: Aleksandar Sekulic, Translational Genomics Research Institute, 445 North Fifth Street, Phoenix, Arizona 85004, USA. E-mail: asekulic@tgen.org

Abbreviations: BCC, basal cell carcinoma; D1, delta 1; D2, delta 2; DEG, differentially expressed gene; FC, fold change; FDA, Food and Drug Administration; FFPE, formalin-fixed, paraffin-embedded; NCBI, National Center for Biotechnology Information; NL, necrobiosis lipoidica; STAT, signal transducer and activator of transcription; TCRD, Target Central Resource Database; Th17, T helper 17; TYK2, tyrosine kinase 2; UR, upstream regulator

Received 7 December 2023; revised 18 March 2024; accepted 8 April 2024; accepted manuscript published online XXX; corrected published online XXX

Cite this article as: JID Innovations 2024;4:100296

initial insights in such approaches represent a significant barrier when attempting to analyze rare disease conditions where appropriate models and abundant patient samples may not be available. As an alternative, causal network analysis (causal reasoning) approaches leverage the continually expanding knowledge of molecular interaction networks to analyze patterns of gene expression and predict the upstream regulators (URs) and their individual activation states without necessitating the generation of additional knowledge (Bradley and Barrett, 2017). Identification of UR drivers of altered gene expression in a disease state by such an approach can provide potential therapeutic targets that might have otherwise been missed by conventional transcriptomic analysis.

Necrobiosis lipoidica (NL) is a rare, chronic inflammatory granulomatous disorder of the skin often associated with diabetes mellitus with no FDA approved treatments (Hashemi et al, 2019; Severson et al, 2022a, 2022b). NL ulcerates in up to 35% of cases, is associated with increased pain (Hines et al, 2023), and has malignant potential if left untreated (Harvey et al, 2022). Current treatment modalities are ineffective, and the underlying molecular drivers are unknown.

In this study, we applied a drug discovery pipeline on the basis of causal reasoning using publicly available resources and demonstrated utility in identifying targetable URs as drivers of aberrant cellular disease processes. We first tested and optimized our approach using psoriasis as a disease model with well-characterized molecular mechanisms and have successfully mapped the disease drivers and effective therapeutic options. We demonstrate that identification of URs is specific to disease context because the identical analysis of noninflammatory tissue, in this case, basal cell carcinoma (BCC), yields a very different set of URs. Subsequently, we applied our approach to map the activation networks in NL, identifying involved UR drivers and selecting corresponding therapeutic interventions. These findings informed drug selection for a successfully completed clinical trial, reported separately (Hwang et al, 2024).

RESULTS

Identification of disease drivers in psoriasis and corresponding therapies

Psoriasis is an ideal test model to predict the URs of disease and identify potential therapeutic targets. Mapping of aberrantly regulated URs provides information that is not contained in the expression data alone because the URs driving the RNA transcription changes may not be differentially expressed themselves. We examined the whole-transcriptome profiles from 2 National Center for Biotechnology Information (NCBI) psoriasis datasets (GSE54456 and GSE121212). The entire transcriptome profiling information for GSE54456 was accessed from previously published, publicly available data (Li et al, 2014). A total of 21,510 mapped transcripts were used in the UR analysis, including 3577 DEGs (1049 upregulated and 2538 downregulated) ($\log_2$ fold change [FC] > 1, $P <$ 10E-6). For GSE121212, we obtained the raw mRNA expression data from NCBI and identified DEGs through DESeq2 R package (Tsoi et al, 2019). A total of 31,364 mapped transcripts were included in the UR analysis, including 4954 DEGs (1794 upregulated and 3160 downregulated) ($\log_2$ FC > 1, $P <$ 10E-6). The list of differentially expressed genes (DEGs) between lesional and control tissue for the GSE121212 psoriasis dataset is provided in Supplementary Table S1. Three publicly available directional gene regulation databases (Omnipath, Signor, and CausalR) were utilized to map the molecular networks and identify URs in psoriasis, using the CausalR analytical package (Materials and Methods and Figure 1). For each psoriasis dataset, we examined 2 UR output depths termed delta 1 (D1) and delta 2 (D2), defining the path length between the nodes in the network, such as an UR and the downstream gene expression. The D1 level is the shortest path length among interacting nodes without known intermediary node involvement. The D2 level represents longer path lengths and indirect associations used for UR prediction. The list of all identified URs for GSE54456 (D1 and D2) and GSE121212 (D1 and D2) is provided in Supplementary Tables S2−5, respectively.

To identify drugs with the potential to target mapped URs, the URs were matched to the Target Central Resource Database (TCRD) (http://juniper.health.unm.edu/tcrd/), which contained 1642 unique drugs with well-annotated mechanism of action at the time of analysis (version 6.7). Matched drugs were filtered to exclude nonsensical drug−target relationships, such as drugs inhibiting URs that were identified as already aberrantly inactivated in disease (Materials and Methods provides the details). To assess the degree of agreement in identification of URs between 2 independent psoriasis datasets ($P < .01$), we used Cohen's kappa test, which indicated substantial agreement at each depth of analysis (Cohen's kappa = 0.61, 98.49% agreement [D1]; 0.67, 96.84% agreement [D2]; 95% confidence interval = 0.67−0.85). Given the substantial agreement across both psoriasis datasets, the set of overlapping URs (Table 1) was used in subsequent analytical steps.

A total of 9 most closely related proximal drug-matched URs at D1 predicted as drivers of molecular changes in both psoriasis datasets were identified, including IL-12B, IFNG, IL-23A, IL-1B, CD274 (PD-L1), CD80, IL-17A, TNF, and IL-12A (Figure 2a). These 9 URs mapped to 19 unique drugs, including adalimumab, certolizumab pegol, etanercept, guselkumab, infliximab, ixekizumab, risankizumab, secukinumab, tildrakizumab, and ustekinumab, representing 10 of the 11 FDA-approved biologics for psoriasis as identified at the time of the study (Figure 2b). Evaluation of a broader network of URs that may indirectly control molecular changes in psoriasis (D2) identified 25 overlapping drug-matched URs, including AKR1B1, CCR5, CD80, EGFR, FGFR3, FGFR4, HRH2, IFNG, IL-12A, IL-12B, IL-1B, IL-23A, IL-6, Jak1, Jak2, Jak3, KIT, MAP2K2, poly [ADP-ribose] polymerase 1, PDE3B, SRC, TACR1, toll-like receptor 7, TNF, and tyrosine kinase 2 (TYK2). These 25 URs mapped to 74 unique drugs, of which 8 are FDA-approved biologics for treatment of psoriasis (Table 1). Drugs targeting CD80, IL-1B, IFNG, IL-12A, IL-12B, IL-1B, IL-23A, and TNF were identified at both depths D1 and D2 results, whereas unique findings at D1 included drugs targeting IL-17A and CD274 (Table 1). Fisher's exact test demonstrated highly significant enrichment of current FDA-approved psoriasis biologics at both D1 (Figure 2d) and D2 (data not shown) (GSE54456: $P =$ 1.42E-

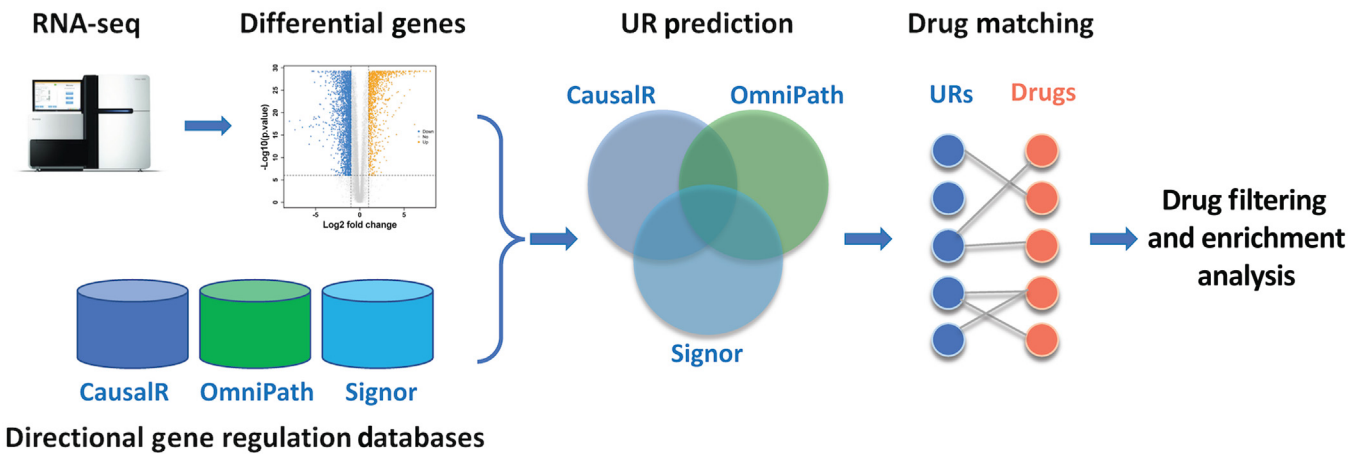

Figure 1. Workflow for identification of URs and matched drugs in cutaneous disease. RNA-seq, RNA sequencing; UR, upstream regulator.

15 and 9.62E-7, respectively; GSE121212: P = 5.13E-12 and 1.56E-6, respectively). Kinase inhibitors were markedly represented, including those targeting Jak1, Jak2, Jak3, TYK2, EGFR, FGFR3, FGFR4, KIT, LYN, MAP2K2, and SRC (Table 1).

Pathway analysis of URs in psoriasis

Pathway analysis was conducted using DAVID (Huang da et al, 2009) to verify known biological processes and pathways of current and potential future therapeutic targets in psoriasis. Deploying Gene Ontology and Kyoto Encyclopedia of Genes and Genomes databases, we conducted pathway analysis using predicted URs for combined D1 and D2 analysis results (D1 + D2) from combined psoriasis datasets. This analysis identified a total of 429 overlapping URs, with 278 predicted to be active and 151 predicted to be inactive ($P < .05$). Pathway analysis on all active URs corroborated functional enrichment of expected outcomes relating to activation of the TNFα–IL-23–T helper 17 (Th17) axis (Rendon and Schäkel, 2019), including chemokine- and cytokine-mediated signaling; Th17 cell differentiation; IL-17 signaling pathway; and other critical inflammatory pathways, including Jak signaling (Figure 3). The 27 most statistically significant URs for combined D1 and D2 results ($P < .01$), which were matched to drugs, mapped similarly to TNFα–IL-23–Th17 axis pathways as well as positive regulation of Jak–signal transducer and activator of transcription (STAT) signaling and Th17 cell differentiation (Figure 2c), in line with current understanding of the molecular pathogenesis in psoriasis.

To ensure that our approach is not biased toward the URs seen in inflammatory conditions, such as psoriasis, we applied the same analytical pipeline to publicly available gene expression data (GSE58375) of BCC, a common skin cancer. Histologically, BCCs are composed predominantly of pathognomonic nests of proliferating tumor cells and, occasionally, a component of immune reaction to neoplastic growth. When compared with psoriasis, our analysis of BCC gene expression yielded a distinct set of URs (Supplementary Tables S6 and S7). Although psoriasis URs mapped predominantly to pathways and processes related to inflammation and immune reaction (Figures 2c and 3), the URs identified in BCC mapped predominantly to noninflammatory pathways (Figure 4), indicating that our approach identifies URs in a disease-specific context.

Transcriptomic profiling and identification of disease drivers in NL

Following the proof of principle in psoriasis, we applied our approach to the study of NL, a disease with poorly understood molecular pathogenesis and paucity of effective therapies. As a discovery set, we analyzed 17 histologically typical, archival formalin-fixed, paraffin-embedded (FFPE) lesions and 5 control tissues. Whole-transcriptome analysis was performed, identifying 3857 DEGs, with 2471 genes upregulated and 1386 genes downregulated in NL ($\log_2$ FC > 1, $P < .05$). Unsupervised clustering of NL transcriptome data highlights global differences between NL diseased tissues and normal skin (Figure 5). A list of all DEGs can be found in Supplementary Table S8.

Using the NL transcriptome data, we carried out UR analysis as described earlier, predicting a total of 565 URs at D1, with 282 being active and 283 inactive ($P < .05$). At D2, a total of 897 predicted URs were identified, with 531 being active and 366 being inactive ($P < .05$). The identified URs (Supplementary Tables S9 and S10) were matched to available drugs using TCRD and filtered as described for psoriasis earlier. A total of 29 URs mapped to 42 drugs at D1, and 68 URs mapped to 156 unique drugs at D2 ($P < .01$) (Table 2). IFNγ and Jaks (Jak1, Jak2, Jak3, TYK2) were among the most significantly activated URs at both depths and mapped to inhibitors of Jak/STAT pathway, including baricitinib, fedratinib, tofacitinib, upadacitinib, and ruxolitinib (Table 2).

Given that only a subset of disease-associated URs may be targetable with existing drugs, we set out to identify the cellular pathways and processes that may be overrepresented within the identified URs in NL. Such information may be relevant for future drug development beyond the agents currently available. To assess the main signaling pathways and processes driving the pathogenesis of NL, pathway analysis using Kyoto Encyclopedia of Genes and Genomes and Gene Ontology was conducted using identified URs for merged depths (D1 + D2). A total of 1094 URs with 592 active and 502 inactive were used ($P < .05$).

Table 1. Table of Overlapping URs and Matched Drugs in Psoriasis ($P < .01$)

Drug Class	Drug Name(s)	UR	Regulation	Depth
Aldose reductase inhibitors	Epalrestat	AKR1B1	+	2
Antiemetics	Aprepitant, fosaprepitant, fosnetupitant, rolapitant	TACR1	+	2
Antimalarials	Hydroxychloroquine	TLR7	+	2
Benzodioxoles	Niperotidine	HRH2	+	2
Bipyridines	Olprinone	PDE3B	+	2
DMARDs	Abatacept	CD80	+	1,2
Expectorants	Choline theophyllinate	PDE3B	+	2
H2 blockers	Cimetidine, ebrotidine, famotidine, nizatidine, ranitidine, roxatidine acetate	HRH2	+	2
HIV entry and fusion inhibitors	Maraviroc	CCR5	+	2
Immunosuppressants	Belatacept	CD80	+	1,2
Inodilators	Pimobendan	PDE3B	+	2
IL antagonists	Rilonacept	IL1B	+	1,2
Jak inhibitors	Baricitinib, ruxolitinib, tofacitinib, upadacitinib	Jak1	+	2
	Baricitinib, fedratinib, ruxolitinib, tofacitinib, upadacitinib	Jak2	+	2
	Upadacitinib, tofacitinib	Jak3	+	2
	Tofacitinib	TYK2	+	2
Kinase inhibitors	Afatinib, dacomitinib, erlotinib, gefitinib, icotinib, lapatinib, neratinib, osimertinib, vandetanib	EGFR	+	2
	Erdafitinib, nintedanib, pazopanib, pemigatinib	FGFR3	+	2
	Nintedanib	FGFR4	+	2
	Avapritinib, cabozantinib, dasatinib, imatinib, lenvatinib, pazopanib, pexidartinib, sunitinib	KIT	+	2
	Bosutinib	LYN	+	2
	Binimetinib, selumetinib, trametinib	MAP2K2	+	2
	Dasatinib	SRC	+	2
mAbs	Atezolizumab, avelumab, durvalumab	CD274	+	1
	Cetuximab, necitumumab	EGFR	+	2
	Emapalumab	IFNG	+	1,2
	Ustekinumab	**IL-12A**	+	1,2
	Guselkumab, tildrakizumab, ustekinumab	**IL-12B**	+	1,2
	Canakinumab	IL-1B	+	1,2
	Ixekizumab, secukinumab	**IL-17A**	+	1
	Guselkumab, risankizumab, tildrakizumab, ustekinumab	**IL-23A**	+	1,2
	Siltuximab	IL-6	+	2
	Adalimumab, **certolizumab pegol**, golimumab, **infliximab**	**TNF**	+	1,2
Naphthalenes	Tolrestat	AKR1B1	+	2
Neurokinin (NK1) Antagonists	Netupitant	TACR1	+	2
PARP inhibitors	Niraparib, olaparib, rucaparib, talazoparib tosylate	PARP1	+	2
Phenylpiperazines	Olmutinib	EGFR	+	2
Phenylpiperidines	Casopitant	TACR1	+	2
Platelet inhibitors	Dipyridamole	PDE3B	+	2
TNF inhibitors	**Etanercept**	**TNF**	+	1,2
Tyrosine Kinase inhibitor, Angiogenesis Inhibitor, VEGF inhibitor	Sorafenib	KIT	+	2
Xanthines	Bufylline	PDE3B	+	2

Abbreviations: PARP, poly [ADP-ribose] polymerase 1; TLR7, toll-like receptor 7; UR, upstream regulator.

Among the top enriched activated pathways, our analysis indicated proinflammatory responses, including increased production of IFNγ and activation of Jak–STAT signaling (Figure 6).

To better understand whether currently druggable URs align with most prominent pathways in NL, we used our merged set of drug-matched URs at (D1 + D2). A total of 66 URs with 61 active and 5 inactive were used ($P < .01$). Pathway analysis on drug-matched URs revealed proinflammatory results similar to the earlier mapping of all URs, highlighting the positive regulation of tyrosine phosphorylation of STAT protein and Jak–STAT signaling pathway as the top 3 pathways most suitable for drug repurposing (Figure 7).

Validation of NL findings on an independent cohort

To independently assess our initial discovery of relevant URs in NL, we carried out a validation study by applying our pipeline to whole-transcriptome data of baseline (untreated) NL disease tissues collected as part of a phase 2 clinical trial measuring efficacy of topical ruxolitinib treatment in NL, reported separately (Hwang et al, 2024). Whole-

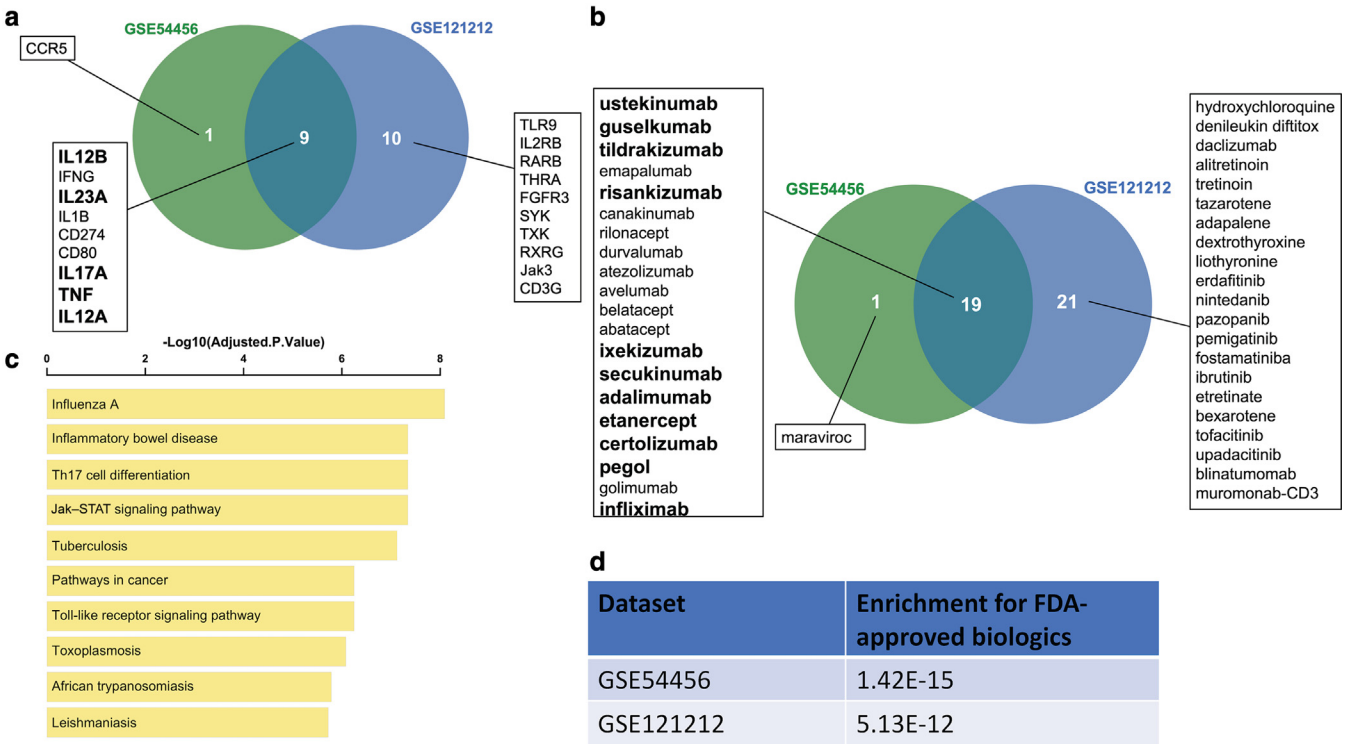

Dataset	Enrichment for FDA-approved biologics
GSE54456	1.42E-15
GSE121212	5.13E-12

Figure 2. Identification of targetable URs involved in the pathogenesis of psoriasis. (**a**) Drug-matched URs (D1; $P < .01$). (**b**) Drugs matched to URs (D1; $P < .1$). (**c**) Top 10 KEGG pathway results for overlapping drug-matched URs (D1 + D2, $P < .01$). (**d**) Enrichment of FDA-approved biologics in psoriasis (D1; $P < .01$). D1, delta 1; D2, delta 2; FDA, Food and Drug Administration; KEGG, Kyoto Encyclopedia of Genes and Genomes; UR, upstream regulator.

transcriptomic analysis was performed on lesional and adjacent normal (control) skin tissue before therapy (n = 12 and 12, respectively). Transcriptomic analysis of 10 NL and 11 healthy skin samples (3 samples removed from analysis as technical outliers) identified 5914 DEGs ($\log_2$ FC > 1, $P <$ .05), of which 3210 were found to be upregulated, and 2704

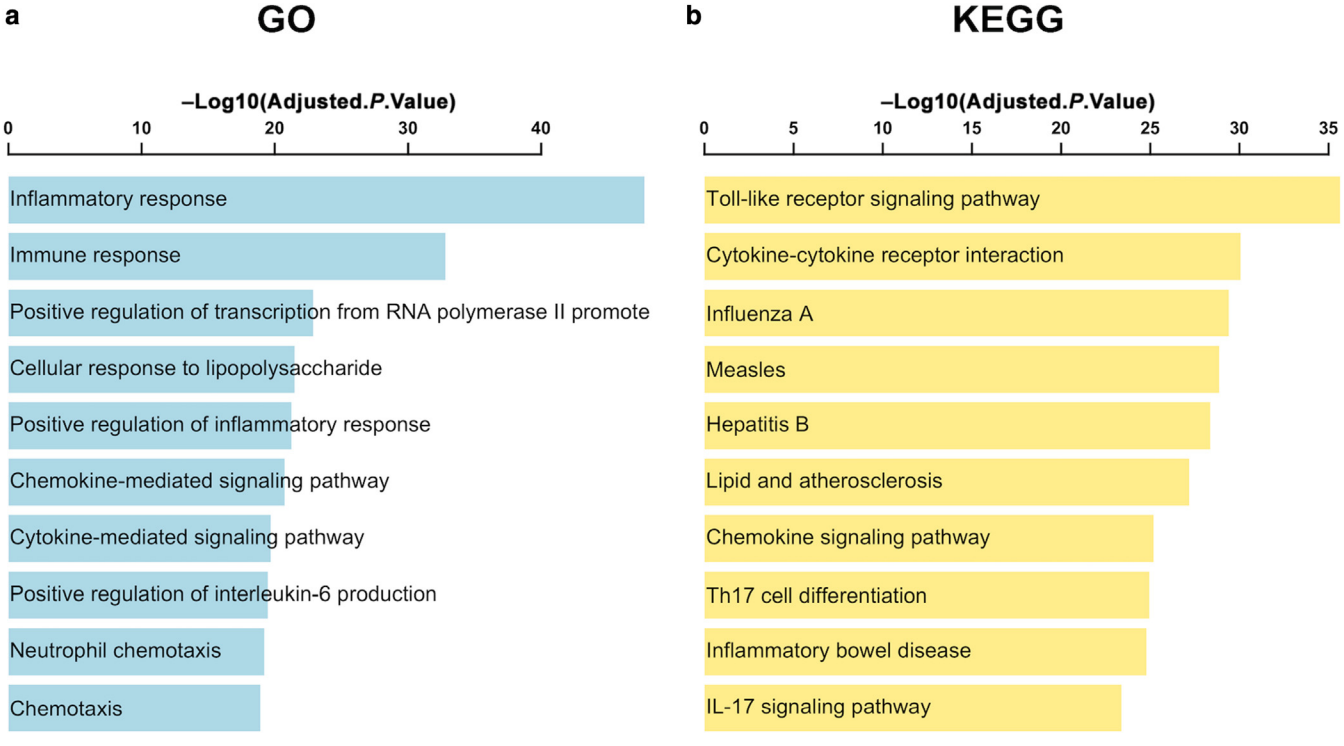

Figure 3. Pathway analysis of all identified URs involved in pathogenesis of psoriasis. (**a**) Top 10 GO pathway results for all overlapping URs (D1 + D2, $P <$ .05). (**b**) Top 10 KEGG pathway results for all overlapping URs (D1 + D2, $P < .05$). D1, delta 1; D2, delta 2; FDA, Food and Drug Administration; GO, Gene Ontology; KEGG, Kyoto Encyclopedia of Genes and Genomes; STAT, signal transducer and activator of transcription; Th17, T helper 17; UR, upstream regulator.

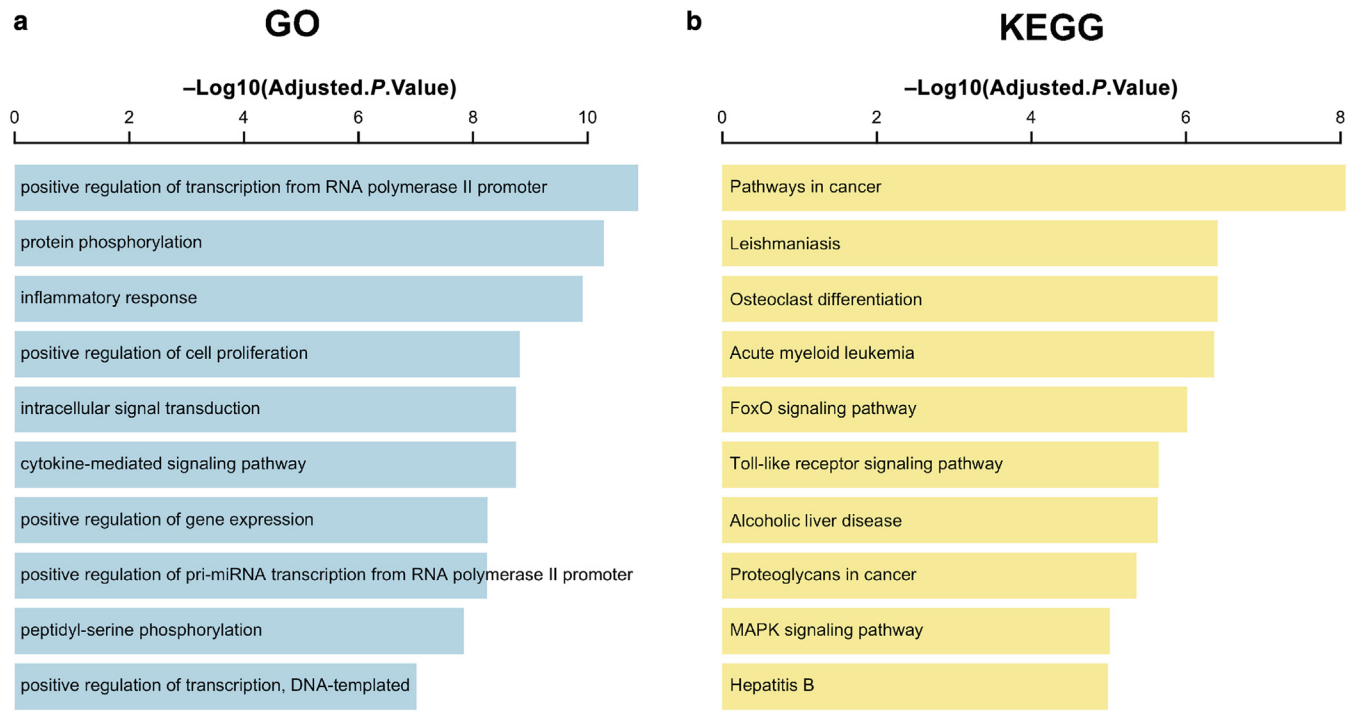

Figure 4. Pathway analysis using all identified URs in BCC. (**a**) Top 10 GO-identified pathways (D1+D2, $P < .05$). (**b**) Top 10 KEGG-identified pathways (D1 + D2, $P < .05$). BCC, basal cell carcinoma; GO, Gene Ontology; KEGG, Kyoto Encyclopedia of Genes and Genomes; UR, upstream regulator.

were downregulated. The list of all DEGs can be found in Supplementary Table S11.

UR analysis on whole-transcriptome data predicted a total of 473 URs at D1 and 705 URs at D2 ($P < .05$), with a final filtered list of 21 URs mapping to 35 unique drugs at D1 and 55 URs mapping to 147 unique drugs at D2 (Table 3) ($P < .01$). Combining all D1- and D2-level data resulted in 879 total URs, with 493 active and 386 inactive URs ($P < .05$). A total of 58 URs (54 active and 4 inactive) were matched to currently available drugs at $P < .01$.

Pathway analysis of all identified and drug-matched URs in our validation cohort supported the findings in the discovery cohort, with enrichment of several key proinflammatory responses, including the Jak–STAT pathway activation among the top-ranking results (Figure 8). Statistical comparisons of drug-matched URs identified at each depth for both NL cohorts demonstrate significant overlap ($P < .01$). At D1, 15 drug-matched URs overlapped across both NL cohorts, corresponding to a 97.25% agreement (Cohen's kappa = 0.58; 95% confidence interval = 0.67–0.85). At D2, 48 total drug-matched URs overlapped across both NL cohorts, corresponding to a 96.3% agreement (Cohen's Kappa = 0.76; 95% confidence interval = 0.67–0.85). Table 4 summarizes the overlap of predicted URs and mapped drugs for both NL cohorts. Among the most significantly overlapping drug-matched URs at combined D1 and D2 depths were IFNγ and all 4 Jaks (Table 4). Assessing the top-ranked URs and matched drugs for practical utility, including the route of administration (systemic vs topical) and risk for adverse events, we prioritized Jaks as potential first targets. These findings offered a support for a clinical study of ruxolitinib in NL, which was recently completed and reported separately (Hwang et al, 2024).

DISCUSSION

In this study, we present and validate a drug identification and repurposing pipeline to identify candidate targetable drivers of disease and corresponding therapies through application of causal reasoning using a combination of open-access resources and transcriptomics data. Our workflow was first tested using 2 published datasets of psoriasis, demonstrating the ability to enrich significantly for current FDA-approved therapies and map known psoriasis targets and pathways, including components of the TNFα–IL-23–Th17 axis, with established role in T-cell–mediated plaque psoriasis (Rendon and Schäkel, 2019). In addition, our pipeline identified emerging candidates for targeted therapy, detecting TYK2 as a driver of disease, which was subsequently approved by the FDA. Furthermore, we identified additional URs, some of which have known roles in inflammation, but which to date remain unexplored in psoriasis, thus providing potential future therapeutics targets.

Our analysis identified relevant URs in a disease-specific context. Although we identified a highly concordant set of URs between the 2 independent psoriasis datasets, subjecting BCC tumor tissue expression data to the same analysis yielded a distinct set of URs that are predominantly mapped on noninflammatory pathways and cellular processes, highlighting those involved in cell growth and proliferation. Our Gene Ontology analysis did identify a minor immune signature in BCC tissues as well, although at much lower statistical significance than in psoriasis or NL. This could be related to the fact that inflammatory reaction in BCC tissues is not uncommon. However, given that our analysis leveraged publicly available BCC expression data, we cannot determine the proportion of BCC samples that may have included

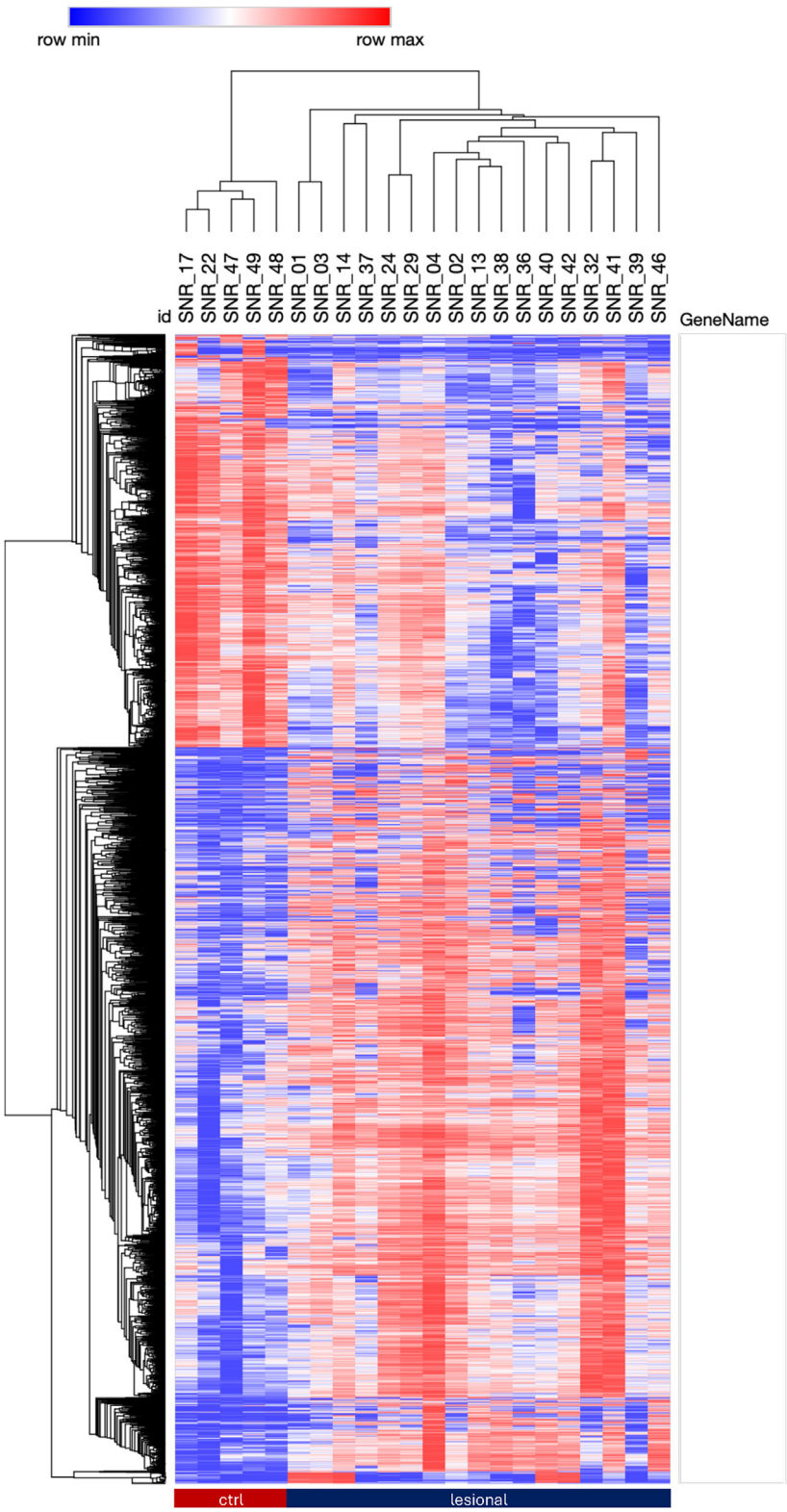

Figure 5. Heatmap illustrating unsupervised clustering of differentially expressed genes between 17 NL and 5 ctrl samples of NL, discovery cohort. $P < .01$; $\log_2$ FC > 1. ctrl, control; FC, fold change; GO, Gene Ontology; NL, necrobiosis lipoidica.

histologic evidence of inflammation. Given the significant increase in the understanding of immune system molecular interactions, it is also possible that such information may be relatively overrepresented in currently available relational databases, resulting in higher sensitivity for identifying such processes.

We applied our approach to a discovery cohort of NL, implicating IFNG activation and the Jak–STAT pathway as a likely driver of disease pathogenesis, and identified inhibition of Jak–STAT pathway as potential therapy. Subsequent analysis of an independent NL cohort further validated our original findings with a reported 97.25 and 96.3% overall

Table 2. Predicted URs and Matched Drugs in NL (Discovery Cohort, $P < .01$)

UR	Regulation	Depth	Drug	Action_Type
ADRB2	+	2	Alprenolol, bopindolol, bupranolol, carteolol, carvedilol, labetalol, levobunolol, metipranolol, nadolol, nebivolol, olodaterol, oxprenolol, penbutolol, propranolol, sotalol, timolol	Antagonist
AGTR1	+	2	Azilsartan medoxomil, candesartan cilexetil, eprosartan, fimasartan, irbesartan, losartan, olmesartan medoxomil, saralasin, tasosartan, telmisartan, valsartan	Antagonist
AKR1B1	+	2	Epalrestat, tolrestat	Inhibitor
ALK	+	2	Alectinib, brigatinib, ceritinib, crizotinib, lorlatinib	Inhibitor
ALOX5	+	2	Balsalazide, benoxaprofen, meclofenamic acid, mesalazine, olsalazine, sulfasalazine, zileuton	Inhibitor
AR	–	2	Danazol, drostanolone propionate, ethylestrenol, fluoxymesterone, mestanolone, methyltestosterone, nandrolone, nandrolone decanoate, nandrolone phenpropionate, oxandrolone, oxymetholone, stanozolol, testosterone, testosterone cypionate, testosterone enantate, testosterone propionate, testosterone undecanoate	Agonist
BTK	+	2	Acalabrutinib, ibrutinib, zanubrutinib	Inhibitor
CCR5	+	2	Maraviroc	Antagonist
CD19	+	2	Blinatumomab	Antibody binding
CD274	+	2	Atezolizumab, avelumab, durvalumab	Antibody binding
CD4	+	1,2	Ibalizumab	Antibody binding
CD79B	+	2	Polatuzumab vedotin	Antibody binding
CD80	+	1,2	Abatacept, belatacept	Inhibitor
CD86	+	1,2	Abatacept, belatacept	Inhibitor
CSF1R	+	1	Pazopanib, pexidartinib, sunitinib	Inhibitor
CSF2RB	+	2	Tagraxofusp	Binding agent
CTSL	+	2	Teicoplanin aglycone	Inhibitor
EGFR	+	2	Afatinib, dacomitinib, erlotinib, gefitinib, icotinib, lapatinib, neratinib, olmutinib, osimertinib, vandetanib	Inhibitor
EGFR	+	2	Cetuximab, necitumumab	Antibody binding
ERBB3	+	2	Tucatinib	Inhibitor
ERBB4	+	2	Afatinib, dacomitinib, neratinib	Inhibitor
FGF23	-	1	Burosumab	Antibody binding
FGFR3	+	2	Erdafitinib, nintedanib, pazopanib, pemigatinib, erdafitinib, nintedanib	Inhibitor
FYN	+	1,2	Dasatinib	Inhibitor
HCK	+	1,2	Bosutinib	Inhibitor
HRH2	+	2	Cimetidine, ebrotidine, famotidine, niperotidine, nizatidine, ranitidine, roxatidine acetate	Antagonist
IFNAR2	+	2	Ropeginterferon alfa-2b	Binding agent
IFNG	+	1,2	Emapalumab	Antibody binding
IGF1R	+	2	Teprotumumab	Antagonist
IL-12A	+	1,2	Ustekinumab	Antibody binding
IL-12B	+	1,2	Guselkumab, tildrakizumab, ustekinumab	Antibody binding
IL-1B	+	1,2	Canakinumab	Antibody binding
IL-1B	+	1,2	Rilonacept	Inhibitor
IL-1R1	+	2	Anakinra	Antagonist
IL-23A	+	1,2	Guselkumab, risankizumab, tildrakizumab, ustekinumab	Antibody binding
IL-2RB	+	1,2	Daclizumab, denileukin diftitox	Antibody binding
IL-2RG	+	2	Daclizumab, denileukin diftitox	Antibody binding
IL-3RA	+	2	Tagraxofusp	Binding agent
IL-4R	+	2	Dupilumab	Antibody binding
IL-5RA	+	2	Benralizumab	Antibody binding
IL-6	+	2	Siltuximab	Antibody binding
ITGB1	+	2	Natalizumab	Antibody binding
ITGB2	+	1	Lifitegrast	Antagonist
ITK	+	1,2	Pazopanib	Inhibitor
Jak1	+	1,2	Baricitinib, ruxolitinib, tofacitinib, upadacitinib	Inhibitor
Jak2	+	2	Baricitinib, fedratinib, ruxolitinib, tofacitinib, upadacitinib	Inhibitor
Jak3	+	1,2	Tofacitinib, upadacitinib	Inhibitor
KIT	+	1,2	Avapritinib, cabozantinib, dasatinib, imatinib, lenvatinib, pazopanib, pexidartinib, sorafenib, sunitinib	Inhibitor
LCK	+	1,2	Dasatinib, pazopanib	Inhibitor
LTK	+	2	Lorlatinib	Inhibitor
LYN	+	1,2	Bosutinib	Inhibitor
MAP2K1	+	2	Binimetinib, cobimetinib, selumetinib, trametinib	Inhibitor
MAP2K2	+	2	Binimetinib, selumetinib, trametinib	Inhibitor

(*continued*)

Table 2. Continued

UR	Regulation	Depth	Drug	Action_Type
NFKB1	+	2	Cepharanthine	Inhibitor
NTRK2	+	2	Larotrectinib, lorlatinib	Inhibitor
PARP1	+	2	Olaparib, rucaparib, talazoparib tosylate	Inhibitor
PDE3B	+	2	Bufylline, choline theophyllinate, dipyridamole, olprinone, pimobendan	Inhibitor
PDGFRB	+	2	Dasatinib, imatinib, nintedanib, pazopanib, sorafenib, sunitinib	Inhibitor
PRKAA1	+	2	Cepharanthine	Inhibitor
PSMB8	+	2	Bortezomib	Inhibitor
PTGER3	−	1	Dinoprostone, misoprostol	Agonist
PTK2	+	2	Lorlatinib	Inhibitor
PTK2B	+	2	Lorlatinib	Inhibitor
RET	+	2	Alectinib, cabozantinib, lenvatinib, sorafenib, sunitinib, vandetanib	Inhibitor
S1PR1	−	1	Fingolimod, ozanimod	Agonist
S1PR1	−	1	Siponimod	Modulator
SRC	+	2	Bosutinib, dasatinib	Inhibitor
SYK	+	1	Fostamatinib	Inhibitor
TACR1	+	2	Aprepitant, casopitant, fosaprepitant, netupitant, rolapitant	Antagonist
TLR7	+	1,2	Hydroxychloroquine	Antagonist
TLR9	+	1,2	Hydroxychloroquine	Antagonist
TNF	+	1,2	Adalimumab, certolizumab pegol, golimumab, infliximab	Antibody binding
TNF	+	1,2	Etanercept	Inhibitor
TNFSF11	+	2	Denosumab	Antibody binding
TNFSF13B	+	1,2	Belimumab	Antibody binding
TXK	+	1,2	Ibrutinib	Inhibitor
TYK2	+	2	Tofacitinib	Inhibitor

Abbreviations: NL, necrobiosis lipoidica; PARP1, poly [ADP-ribose] polymerase 1; TLR, toll-like receptor; TYK2, tyrosine kinase 2; UR, upstream regulator.

agreement (D1 and D2 depths, respectively) of drug-matched URs, including the regulators of Jak–STAT pathway signaling. This supports recent anecdotal observations of the efficacy of Jak–STAT inhibitors in NL (Damsky et al, 2020; McPhie et al, 2021; Nugent et al, 2022). Taken together, our work in psoriasis and NL supports the utility of our approach to identify effective candidate targets and matching therapies for application in inflammatory cutaneous diseases and potentially other disorders where well-characterized, targetable pathways may be mediating disease pathogenesis. Finally, our data indicate that archival FFPE specimens can be used for this type of analysis because we demonstrated high concordance of results between our FFPE discovery set and the fresh-frozen tissue validation set. This is particularly attractive when working with rare conditions where fresh-frozen tissues may be hard to access, Our approach has several limitations. The open-access resources have expanding but still incomplete coverage of gene regulation and drug–target relationships. Despite successful identification of 10 of 11 FDA-approved biologics in the psoriasis validation cohort, our method did not identify brodalumab. Although brodalumab is included in TCRD as targeting IL-17RA, none of the 3 relational databases contained information regarding the specific regulation of IL-17RA. Consequently, IL-17R was not flagged as a UR and was not matched to brodalumab. Other IL-17 inhibitors such as ixekizumab and secukinumab were successfully identified among top-ranking psoriasis results. In addition, although TYK2 was successfully identified as a candidate for therapeutic intervention across both psoriasis datasets, deucravacitinib, a recently approved treatment for moderate-to-severe plaque psoriasis, was not identified because it was not included as part of the TCRD drug–target database at the time of this study. Literature-based searches were necessary in supplementing the database limitations. Finally, causal reasoning–based UR prediction relies on the knowledge base of well-established and documented directional gene regulations; thus, our pipeline cannot identify targetable drivers of potential unknown biological processes.

We have demonstrated successful identification of candidate druggable drivers and corresponding therapies in 2 different dermatologic diseases, including 1 rare disease. Our method provides a unique opportunity to the study of other rare diseases in dermatology and beyond. With improved understanding of molecular networks, concomitant increase in the scope and accuracy of relational databases, and increasing numbers of available drugs with annotated mechanism of action, the accuracy and value of our approach are expected to improve over time.

MATERIALS AND METHODS

Sample selection and preparation

Psoriasis. Previously published psoriasis gene expression data were obtained from the NCBI Gene Expression Omnibus database for 2 datasets: GSE54456 (Greenberg et al, 2020; Li et al, 2014; Liang et al, 2017; Tsoi et al, 2015), including 92 psoriasis cases and 82 healthy controls, and GSE121212 (Tsoi et al, 2019). GSE54456 contained 28 psoriasis samples and 38 healthy controls.

BCC. Previously published BCC expression data were obtained from the NCBI Gene Expression Omnibus database for GSE58375 (Atwood et al, 2015), including 13 BCC cases and 8 healthy controls.

NL: discovery cohort. A database search across 3 Mayo Clinic sites (Rochester, Arizona, and Florida) identified 42 cases of active NL and 11 unmatched control FFPE tissues. All cases were verified for diagnosis of NL clinically by a dermatologist and histopathologically by 2 board-certified dermatopathologists (SAN and DJD). A total of 18 NL and 5 control samples produced high-quality RNA-sequencing libraries and were included in RNA-sequencing analysis. One sample was removed as outlier through principal component analysis owing to low read depth (8 million reads), and 17 cases and 5 controls were utilized for downstream analyses.

NL: validation cohort. Tissue biopsies were obtained from patients in a pilot clinical trial (n = 24, reported separately). Punch biopsies (3 mm) of NL lesions and adjacent normal skin at baseline

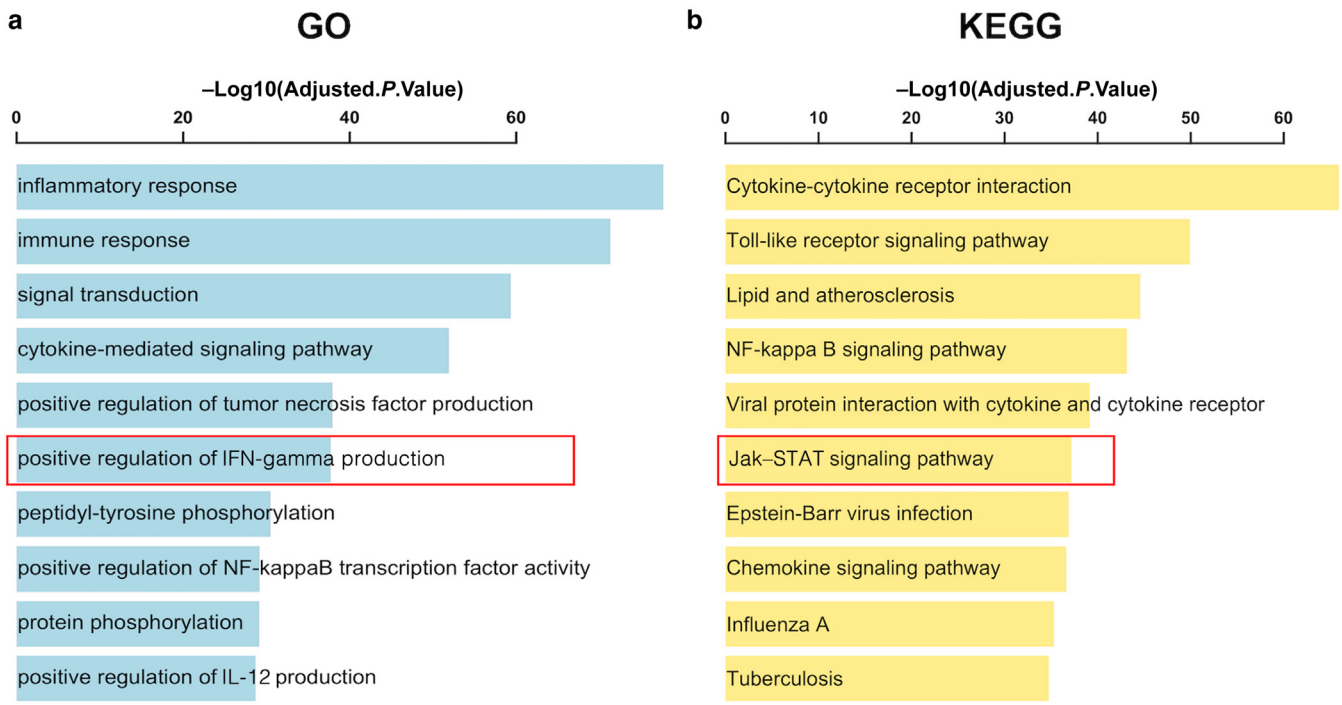

Figure 6. Pathway analysis using all identified URs in NL, discovery cohort. (**a**) Top 10 GO-identified pathways (D1 + D2, $P < .05$). (**b**) Top 10 KEGG-identified pathways (D1 + D2, $P < .05$). GO, Gene Ontology; KEGG, Kyoto Encyclopedia of Genes and Genomes; NL, necrobiosis lipoidica; STAT, signal transducer and activator of transcription; UR, upstream regulator.

were flash frozen and utilized for RNA isolation and transcriptomic sequencing. Two lesional samples and 1 control sample were removed from transcriptomic analyses as outlier samples because of histologically subtle disease and inadequate sample volume. A total of 10 lesional and 11 healthy control samples were utilized for downstream analyses.

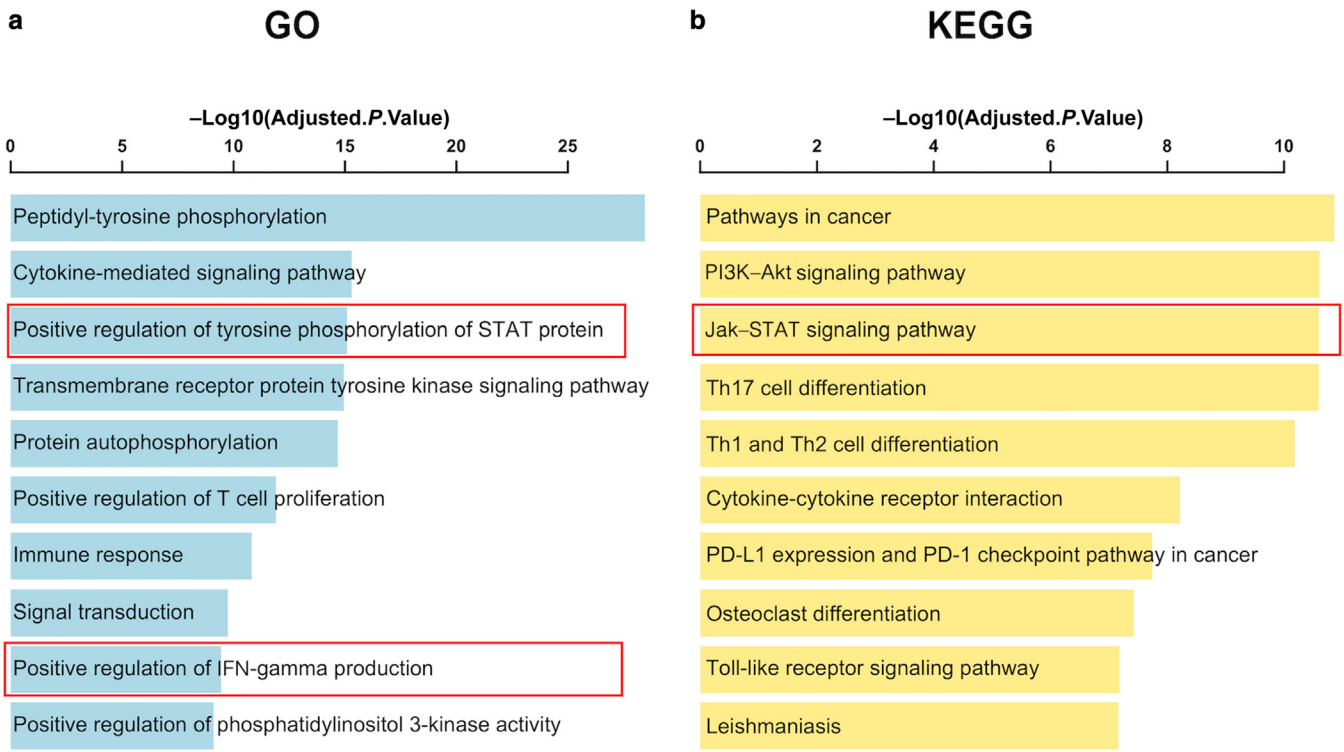

Figure 7. Mapping of drug-matched URs in NL discovery cohort to biological pathways and processes. (**a**) Top 10 GO pathway results for drug-matched URs (D1 + D2, $P < .01$). (**b**) Top 10 KEGG pathway results for drug-matched URs (D1 + D2, $P < .01$). Akt, protein kinase B; GO, Gene Ontology; KEGG, Kyoto Encyclopedia of Genes and Genomes; NL, necrobiosis lipoidica; PI3K, phosphoinositide 3-kinase; STAT, signal transducer and activator of transcription; Th, T helper; UR, upstream regulator.

Table 3. Predicted URs and Matched Drugs in NL (Validation Cohort, $P < .01$)

UR	Regulation	Depth	Drug	Action_Type
ADORA3	+	2	Bufylline, choline theophyllinate, theophylline	Antagonist
ADORA3	+	2	Fostamatinib	Inhibitor
ADRA2B	+	2	Phenoxybenzamine, phentolamine, tolazoline, yohimbine	Antagonist
ADRB2	+	2	Alprenolol, bopindolol, bupranolol, carteolol, carvedilol, labetalol, levobunolol, metipranolol, nadolol, nebivolol, olodaterol, oxprenolol, penbutolol, propranolol, sotalol, timolol	Antagonist
AGTR1	+	2	Azilsartan medoxomil, candesartan cilexetil, eprosartan, fimasartan, irbesartan, losartan, olmesartan medoxomil, saralasin, tasosartan, telmisartan, valsartan	Antagonist
AKR1B1	+	2	Epalrestat, tolrestat	Inhibitor
ALOX5	+	2	Balsalazide, benoxaprofen, meclofenamic acid, mesalazine, olsalazine, sulfasalazine, zileuton	Inhibitor
BTK	+	2	Acalabrutinib, ibrutinib, zanubrutinib	Inhibitor
CCR5	+	2	Maraviroc	Antagonist
CD19	+	1,2	Blinatumomab	Antibody binding
CD274	+	1,2	Atezolizumab, avelumab, durvalumab	Antibody binding
CD4	+	1,2	Ibalizumab	Antibody binding
CD79B	+	2	Polatuzumab vedotin	Antibody binding
CD80	+	1,2	Abatacept, belatacept	Inhibitor
CD86	+	1,2	Abatacept, belatacept	Inhibitor
CHRM4	-	1	Aclatonium	Agonist
CSF2RB	+	2	Tagraxofusp	Binding agent
CTSL	+	1,2	Teicoplanin aglycone	Inhibitor
EGFR	+	2	Afatinib, dacomitinib, erlotinib, gefitinib, icotinib, lapatinib, neratinib, olmutinib, osimertinib, vandetanib	Inhibitor
EGFR	+	2	Cetuximab, necitumumab	Antibody binding
ERBB4	+	2	Afatinib, dacomitinib, neratinib	Inhibitor
FGFR3	+	2	Erdafitinib, nintedanib, pazopanib, pemigatinib	Inhibitor
FGFR4	+	2	Erdafitinib, nintedanib	Inhibitor
HRH2	+	2	Cimetidine, ebrotidine, famotidine, niperotidine, nizatidine, ranitidine, roxatidine acetate	Antagonist
IFNG	+	1,2	Emapalumab	Antibody binding
IL-12A	+	1,2	Ustekinumab	Antibody binding
IL-12B	+	1,2	Guselkumab, tildrakizumab, ustekinumab	Antibody binding
IL-1B	+	1,2	Canakinumab	Antibody binding
IL-1B	+	1,2	Rilonacept	Inhibitor
IL-2RB	+	1,2	Daclizumab, denileukin diftitox	Antibody binding
IL-2RG	+	2	Daclizumab, denileukin diftitox	Antibody binding
IL-3RA	+	2	Tagraxofusp	Binding agent
IL-4R	+	2	Dupilumab	Antibody binding
IL-5RA	+	2	Benralizumab	Antibody binding
IL-6ST	+	2	Sarilumab, tocilizumab	Antibody binding
ITGB1	+	2	Natalizumab	Antibody binding
ITK	+	1,2	Pazopanib	Inhibitor
Jak1	+	2	Baricitinib, ruxolitinib, tofacitinib, upadacitinib	Inhibitor
Jak2	+	2	Baricitinib, fedratinib, ruxolitinib, tofacitinib, upadacitinib	Inhibitor
Jak3	+	2	Tofacitinib, upadacitinib	Inhibitor
KDR	+	2	Apatinib, axitinib, cabozantinib, erdafitinib, lenvatinib, nintedanib, pazopanib, regorafenib, sorafenib, sunitinib, tivozanib, vandetanib	Inhibitor
KDR	+	2	Ramucirumab	Antibody binding
KIT	+	2	Avapritinib, cabozantinib, dasatinib, imatinib, lenvatinib, pazopanib, pexidartinib, sorafenib, sunitinib	Inhibitor
LCK	+	1,2	Dasatinib, pazopanib	Inhibitor
LYN	+	1,2	Bosutinib	Inhibitor
MAP2K1	+	2	Binimetinib, cobimetinib, selumetinib, trametinib	Inhibitor
MAP2K2	+	2	Binimetinib, selumetinib, trametinib	Inhibitor
NFKB1	+	2	Cepharanthine	Inhibitor
P2RY12	+	2	Cangrelor, clopidogrel, prasugrel, ticlopidine	Antagonist
PARP1	+	2	Niraparib, olaparib, rucaparib, talazoparib tosylate	Inhibitor
PDE3B	+	2	Bufylline, choline theophyllinate, dipyridamole, olprinone, pimobendan	Inhibitor
PTK2	+	2	Lorlatinib	Inhibitor

Table 3. Continued

UR	Regulation	Depth	Drug	Action_Type
RARG	–	1	Acitretin, adapalene, alitretinoin, tazarotene, tretinoin, trifarotene	Agonist
RXRG	–	2	Alitretinoin, bexarotene, etretinate	Agonist
SRC	+	2	Bosutinib, dasatinib	Inhibitor
SYK	+	1	Fostamatinib	Inhibitor
TACR1	+	2	Aprepitant, casopitant, fosaprepitant, netupitant, rolapitant	Antagonist
THRA	–	1,2	Dextrothyroxine, liothyronine	Agonist
TLR7	+	1,2	Hydroxychloroquine	Antagonist
TLR9	+	1,2	Hydroxychloroquine	Antagonist
TNF	+	1,2	Adalimumab, certolizumab pegol, golimumab, infliximab	Antibody binding
TNF	+	1,2	Etanercept	Inhibitor
TYK2	+	2	Tofacitinib	Inhibitor

Abbreviations: NL, necrobiosis lipoidica; PARP1, poly [ADP-ribose] polymerase 1; TLR, toll-like receptor; TYK2, tyrosine kinase 2; UR, upstream regulator.

RNA library preparation and sequencing

NL. For the NL discovery cohort samples, paraffin was removed using Citrisolv, and RNA was isolated from 5 × 10 μm FFPE tissue sections, using the QIAcube instrument and Qiagen miRNeasy FFPE Kit, following manufacturer's instructions. RNA-sequencing libraries were constructed from 100 ng of quality-controlled RNA (Agilent Tapestation) using the Illumina TruSeq RNA Access kit. The initial library construction used 17 cycles of PCR amplification after ligation of full-length sequencing adaptors, and exon enrichment was performed as 4-plex reactions with 200 ng of each respective library. All other steps followed the manufacturer's instructions. Each pool of 4 enriched RNA-sequencing libraries were sequenced on a single Illumina HiSeq4000 flow cell using an 82 × 82 paired end read format, and FASTQ files were generated using bcl2fastq, version 2.18.0.12 (Illumina). Fresh-frozen tissues from the NL validation cohort were processed, sequenced, and analyzed through standard RNA pipeline (Kalari et al, 2014).

Transcriptomic analysis

Psoriasis data analysis. The entire transcriptome profiling information for GSE54456, including up and downregulated genes, was accessed from previously published, publicly available data (Li et al, 2014). A total of 21,510 mapped transcripts were used in the UR analysis, including 3577 DEGs (1049 upregulated and 2538 downregulated) ($\log_2$ FC > 1, P < 10E-6). For GSE121212, we obtained the raw mRNA expression data from NCBI and identified DEGs through DESeq2 R package (Tsoi et al, 2019). A total of 31,364 mapped transcripts were included in the UR analysis, including 4954 DEGs (1794 upregulated and 3160 downregulated) ($\log_2$ FC > 1, P < 10E-6).

BCC data analysis. The counts data for this study were acquired through the recount2 package in R (Collado-Torres et al, 2017), leveraging its extensive repository housing >70,000 uniformly processed human RNA-sequencing samples sourced from The Cancer Genome Atlas, Sequence Read Archive, and Genotype-Tissue Expression datasets. After downloading and loading the RangedSummarizedExperiment (rse) object into R, the counts data were accessed using the command assays(rse)$counts. This approach enabled the retrieval of comprehensive coverage count matrices essential for downstream analysis in the study. A total of 1760 DEGs (1164 upregulated and 596 downregulated) were identified through DESeq2 analysis ($\log_2$ FC > 1, adjusted P < .05). One normal sample was removed as an outlier on the basis of principal component analysis.

NL data analysis. Whole-transcriptome analysis was performed, and reads were aligned to the NCBI Build 38 reference genome (hg38) using MAPRSeq 3.0, with an average mapping rate of 93.59 ± 2.47% (mean ± SD) in the discovery cohort and 94.02 ± 1.60% (mean ± SD) in the validation cohort. Gene expression levels were obtained for 40,760 genes/transcripts annotated in the RefSeq database in the discovery cohort and 38,645 in the validation cohort. Obtained gene expression levels were used as input for downstream UR analysis. For both NL cohorts, differential gene expression (DEG) analysis was conducted using DESeq2 R package (Love et al, 2014), with criteria for significant DEGs assigned as $\log_2$ FC > 1 and P < .05 after adjusting for false discovery rate.

UR analysis and drug matching

For both psoriasis and NL cohorts, whole-transcriptome profiles were assigned a trinary code to indicate directionality on the basis of differential gene expression analysis (+1, 0, −1 representing upregulated, no change, and downregulated, respectively). Annotated directional gene regulation relationships (in the format of .sif files) from 3 publicly available gene regulation databases/sources—Omnipath (OmnipathR_2.0.0) (Türei et al, 2016), SignoR (version 2.0) (Perfetto et al, 2016), and CausalR (Bradley and Barrett, 2017)—were utilized in UR prediction through application of the CausalR (CausalR_1.22.0) software package (Bradley and Barrett, 2017). Two depths of predicted URs were considered for downstream analysis: D1, which utilizes direct gene regulation associations with the shortest path length to inform UR prediction, and D2, including a broader network of indirect associations.

Meta analysis using metaRNASeq_1.0.3 was performed on UR data from all 3 database outputs at each depth to assess overall significance (Rau et al, 2014). The resulting D1 and D2 UR lists were filtered for significance (Fisher's combined P < .01) and drug matched using MySQL Workbench (https://www.mysql.com/products/workbench/) and the TCRD (version 6.7.0) (Oprea et al, 2018; Sheils et al, 2021). Drug matches were manually filtered for accuracy through comparisons of UR activation state and drug activity, and resulting erroneous matches with no clinical utility were removed (ie, all null drug activities, activated UR mapped to agonist, inactive UR mapped to antagonist, etc). Cohen's Kappa statistical test was used to assess agreement across psoriasis and NL cohorts for drug-matched URs identified at each depth of the analysis.

Pathway analysis

Gene function and pathway enrichment analyses based on Gene Ontology terms and Kyoto Encyclopedia of Genes and Genomes pathway were performed using DAVID (Huang da et al, 2009) to identify significantly enriched pathways associated with active URs for D1- and D2-merged results on all or drug-matched URs. For psoriasis, pathway analysis was performed on the overlap of all URs (Fisher's combined P < .05) and drug-matched URs across both

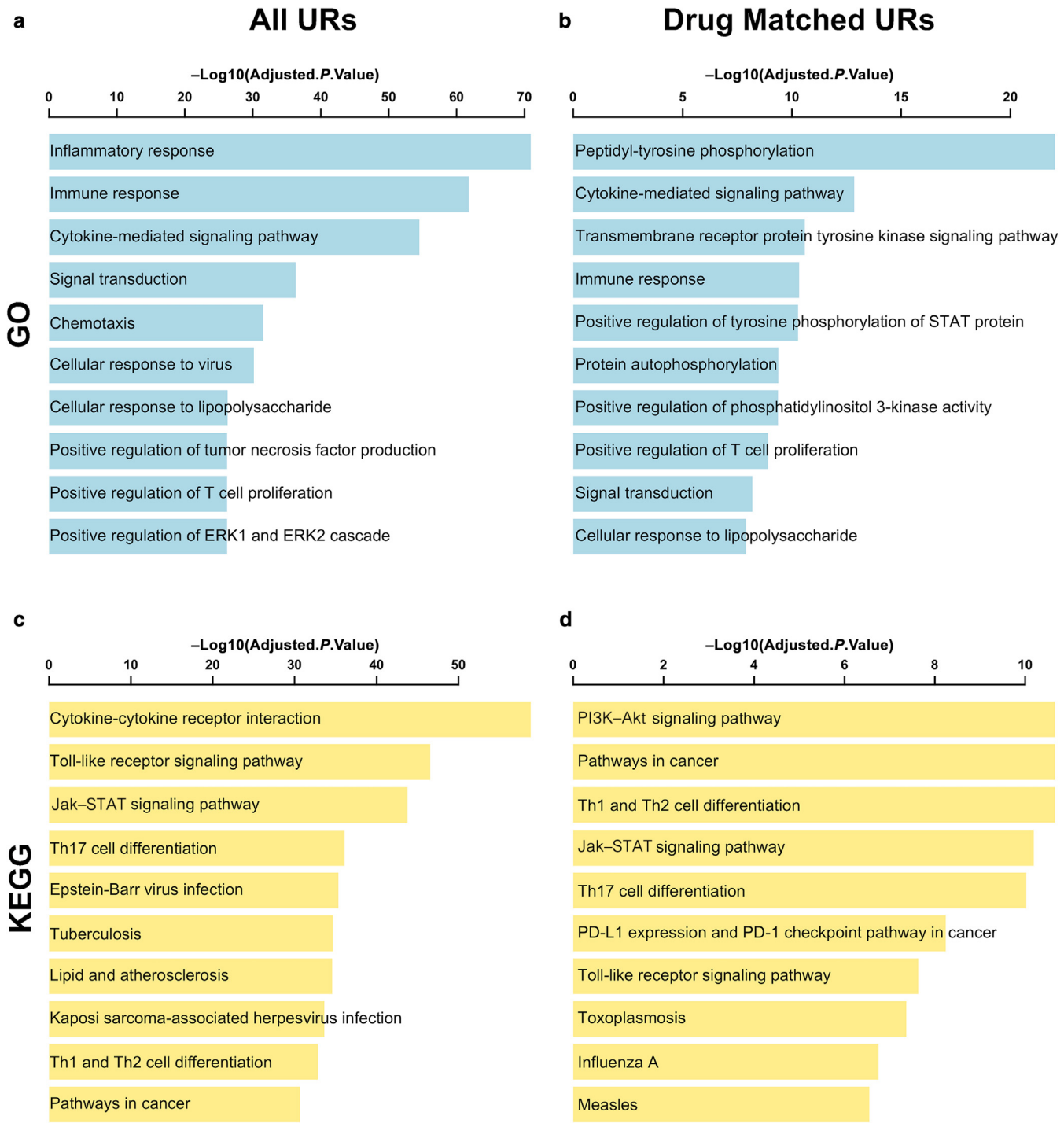

Figure 8. Pathway analysis of all identified and drug-matched upstream regulators involved in pathogenesis of NL, validation cohort. (**a**) Top 10 GO pathway results for all identified URs (D1 + D2, $P < .05$). (**b**) Top 10 GO pathway results for drug-matched URs (D1 + D2, $P < .01$). (**c**) Top 10 KEGG pathway results for all identified URs (D1 + D2, $P < .05$). (**d**) Top 10 KEGG pathway results for drug-matched URs (D1 + D2, $P < .01$). Akt, protein kinase B; GO, Gene Ontology; KEGG, Kyoto Encyclopedia of Genes and Genomes; NL, necrobiosis lipoidica; PI3K, phosphoinositide 3-kinase; STAT, signal transducer and activator of transcription; Th, T helper; UR, upstream regulator.

datasets (Fisher's combined $P < .01$). For BCC, pathway analysis was performed on the overlap of all URs (Fisher's combined $P < .05$). For NL cohorts, data were analyzed for each dataset separately. Pathway analysis was performed on all URs (Fisher's combined $P < .05$) and drug-matched URs identified at combined depths (Fisher's combined $P < .01$).

Enrichment calculations

To assemble the list of FDA-approved psoriasis drugs for enrichment calculations, we performed searches on the FDA database. Most drugs were exported from FDALabel by selecting Human RX as labeling types as well as by selecting simple search, psoriasis, and indications and usage. The resulting drug list was deduplicated and

Table 4. Table of Overlapping URs and Matched Drugs in NL ($P < .01$)

UR	Regulation	Depth	Drug	Action_Type
ADRB2	+	2	Alprenolol, bopindolol, bupranolol, carteolol, carvedilol, labetalol, levobunolol, metipranolol, nadolol, nebivolol, olodaterol, oxprenolol, penbutolol, propranolol, sotalol, timolol	Antagonist
AGTR1	+	2	Azilsartan medoxomil, candesartan cilexetil, eprosartan, fimasartan, irbesartan, losartan, olmesartan medoxomil, saralasin, tasosartan, telmisartan, valsartan	Antagonist
AKR1B1	+	2	Epalrestat, tolrestat	Inhibitor
ALOX5	+	2	Balsalazide, benoxaprofen, meclofenamic acid, mesalazine, olsalazine, sulfasalazine, zileuton	Inhibitor
BTK	+	2	Acalabrutinib, ibrutinib, zanubrutinib	Inhibitor
CCR5	+	2	Maraviroc	Antagonist
CD19	+	2	Blinatumomab	Antibody binding
CD274	+	2	Atezolizumab, avelumab, durvalumab	Antibody binding
CD4	+	1,2	Ibalizumab	Antibody binding
CD79B	+	2	Polatuzumab vedotin	Antibody binding
CD80	+	1,2	Abatacept, belatacept	Inhibitor
CD86	+	1,2	Abatacept, belatacept	Inhibitor
CSF2RB	+	2	Tagraxofusp	Binding agent
CTSL	+	2	Teicoplanin aglycone	Inhibitor
EGFR	+	2	Afatinib, dacomitinib, erlotinib, gefitinib, icotinib, lapatinib, neratinib, olmutinib, osimertinib, vandetanib	Inhibitor
EGFR	+	2	Cetuximab, necitumumab	Antibody binding
ERBB4	+	2	Afatinib, dacomitinib, neratinib	Inhibitor
FGFR3	+	2	Erdafitinib, nintedanib, pazopanib, pemigatinib	Inhibitor
FGFR4	+	2	Erdafitinib, nintedanib	Inhibitor
HRH2	+	2	Cimetidine, ebrotidine, famotidine, niperotidine, nizatidine, ranitidine, roxatidine acetate	Antagonist
IFNG	+	1,2	Emapalumab	Antibody binding
IL-12A	+	1,2	Ustekinumab	Antibody binding
IL-12B	+	1,2	Guselkumab, tildrakizumab, ustekinumab	Antibody binding
IL-1B	+	1,2	Canakinumab	Antibody binding
IL-1B	+	1,2	Rilonacept	Inhibitor
IL-2RB	+	1,2	Daclizumab, denileukin diftitox	Antibody binding
IL-2RG	+	2	Daclizumab, denileukin diftitox	Antibody binding
IL-3RA	+	2	Tagraxofusp	Binding agent
IL-4R	+	2	Dupilumab	Antibody binding
IL-5RA	+	2	Benralizumab	Antibody binding
ITGB1	+	2	Natalizumab	Antibody binding
ITK	+	1,2	Pazopanib	Inhibitor
Jak1	+	2	Baricitinib, ruxolitinib, tofacitinib, upadacitinib	Inhibitor
Jak2	+	2	Baricitinib, fedratinib, ruxolitinib, tofacitinib, upadacitinib	Inhibitor
Jak3	+	2	Tofacitinib, upadacitinib	Inhibitor
KIT	+	2	Avapritinib, cabozantinib, dasatinib, imatinib, lenvatinib, pazopanib, pexidartinib, sorafenib, sunitinib	Inhibitor
LCK	+	1,2	Dasatinib, pazopanib	Inhibitor
LYN	+	1,2	Bosutinib	Inhibitor
MAP2K1	+	2	Binimetinib, cobimetinib, selumetinib, trametinib	Inhibitor
MAP2K2	+	2	Binimetinib, selumetinib, trametinib	Inhibitor
NFKB1	+	2	Cepharanthine	Inhibitor
PARP1	+	2	Niraparib, olaparib, rucaparib, talazoparib tosylate	Inhibitor
PDE3B	+	2	Bufylline, choline theophyllinate, dipyridamole, olprinone, pimobendan	Inhibitor
PTK2	+	2	Lorlatinib	Inhibitor
SRC	+	2	Bosutinib, dasatinib	Inhibitor
SYK	+	1	Fostamatinib	Inhibitor
TACR1	+	2	Aprepitant, casopitant, fosaprepitant, netupitant, rolapitant	Antagonist
TLR7	+	1,2	Hydroxychloroquine	Antagonist
TLR9	+	1,2	Hydroxychloroquine	Antagonist
TNF	+	1,2	Adalimumab, certolizumab pegol, golimumab, infliximab	Antibody binding
TNF	+	1,2	Etanercept	Inhibitor
TYK2	+	2	Tofacitinib	Inhibitor

Abbreviations: NL, necrobiosis lipoidica; PARP1, poly [ADP-ribose] polymerase 1; TLR, toll-like receptor; TYK2, tyrosine kinase 2; UR, upstream regulator.

corrected for erroneous matches. All drugs with general FDA approval and all drug combinations were excluded. Any additional FDA-approved drugs from psoriasis.org were included, resulting in a final list of 30 FDA-approved drugs for treatment of psoriasis at the time of the study. For biologics with defined mechanism of action, we focused this list to include a total of 11 approved biologics. All

filtered drug matches identified for psoriasis cohorts at each depth (Fisher's combined $P < .01$) were compared with this list of biologics to assess overall enrichment through application of the Fisher's exact statistical test.

ETHICS STATEMENT

This study was performed in accordance with the Declaration of Helsinki and the Nurenberg Code. Collection of human tissue samples for this study was approved as part of the study protocol. This human study was approved by Mayo Clinic Institutional Review Board. Written, informed consent was obtained from all patients and control participants.

DATA AVAILABILITY STATEMENT

Dataset related to this article can be found at National Center for Biotechnology Information Gene Expression Omnibus database with Accession number GSE267132: https://www.ncbi.nlm.nih.gov/geo/query/acc.cgi?acc=GSE267132).

ORCIDs

Xing Li: http://orcid.org/0000-0002-8541-8363
Julia S. Lehman: http://orcid.org/0000-0002-7389-3853
Steven A. Nelson: http://orcid.org/0000-0003-2240-6397
David J. DiCaudo: http://orcid.org/0000-0001-8088-9353
Rekha Mudappathi: http://orcid.org/0000-0001-7965-0919
Angelina Hwang: http://orcid.org/0000-0001-8769-2916
Jacob Kechter: http://orcid.org/0000-0002-2646-0166
Mark R. Pittelkow: http://orcid.org/0000-0001-7913-0294
Aaron R. Mangold: http://orcid.org/0000-0001-6873-1705
Aleksandar Sekulic: http://orcid.org/0000-0002-1323-3220

CONFLICT OF INTEREST

ARM consults for Incyte (current), Clarivate (past), Boehringer Ingelheim (past), and Janssen Global Services LLC (current); is a research investigator for miRagen Therapeutics (past), Incyte (current), Corbus Pharmaceuticals (past), Regeneron Pharmaceuticals (current), Solgenix (past), Eli Lilly and Company (current), Pfizer (current), arGEN-X (current), Kyowa Kirin (current), Merck (current), and Priovant (current); is on advisory board for Kyowa Hakko Kirin Pharma (current), Momenta Pharmaceuticals (past), Eli Lilly and Company (current), Regeneron Pharmaceuticals (current), and PHLECS (past). The remaining authors state no conflict of interest.

ACKNOWLEDGMENTS

The authors are thankful to Nicholas Page for providing support for this work. Funding was provided by the Mayo Clinic.

AUTHOR CONTRIBUTIONS

Conceptualization: AS; Data Curation: XL, AH, JSL, DJD, SAN, RM; Formal Analysis: XL, AH, RM; Funding Acquisition: AS; Investigation: AS; Methodology: AS, XL, AH, RM; Project Administration: AS; Resources: AS, AH, XL, JSL, SAN; Software: XL, RM; Supervision: AS; Validation: XL; Visualization: XL, AH; Writing- Original Draft Preparation: AH; Writing- Review and Editing: AS, AH, XL, JK, AH, ARM, MRP, JSL, DJD, SAN, RM

DECLARATION OF ARTIFICIAL INTELLIGENCE (AI) AND LARGE LANGUAGE MODELS (LLM)

The author(s) did not use AI/LLM in any part of the research process and/or manuscript preparation.

SUPPLEMENTARY MATERIAL

Supplementary material is linked to the online version of the paper at www.jidonline.org, and at https://doi.org/10.1016/j.xjidi.2024.100296.

REFERENCES

Atwood SX, Sarin KY, Whitson RJ, Li JR, Kim G, Rezaee M, et al. Smoothened variants explain the majority of drug resistance in basal cell carcinoma. Cancer Cell 2015;27:342–53.

Bradley G, Barrett SJ. CausalR: extracting mechanistic sense from genome scale data. Bioinformatics 2017;33:3670–2.

Collado-Torres L, Nellore A, Kammers K, Ellis SE, Taub MA, Hansen KD, et al. Reproducible RNA-seq analysis using recount2. Nat Biotechnol 2017;35:319–21.

Damsky W, Singh K, Galan A, King B. Treatment of necrobiosis lipoidica with combination Janus kinase inhibition and intralesional corticosteroid. JAAD Case Rep 2020;6:133–5.

Dowden H, Munro J. Trends in clinical success rates and therapeutic focus. Nat Rev Drug Discov 2019;18:495–6.

Fetro C, Scherman D. Drug repurposing in rare diseases: myths and reality. Therapie 2020;75:157–60.

Greenberg EN, Marshall ME, Jin S, Venkatesh S, Dragan M, Tsoi LC, et al. Circadian control of interferon-sensitive gene expression in murine skin. Proc Natl Acad Sci U S A 2020;117:5761–71.

Harvey JA, Severson KJ, Brumfiel CM, Patel MH, Butterfield RJ, Nelson SA, et al. Necrobiosis lipoidica-associated cutaneous malignancy. J Am Acad Dermatol 2022;86:1428–9.

Hashemi DA, Brown-Joel ZO, Tkachenko E, Nelson CA, Noe MH, Imadojemu S, et al. Clinical features and comorbidities of patients with necrobiosis lipoidica with or without diabetes. JAMA Dermatol 2019;155:455–9.

Hines A, Butterfield R, Boudreaux B, Bhullar P, Severson KJ, McBane RD, et al. Characteristics of ulcerated and non-ulcerated necrobiosis lipoidica. Int J Dermatol 2023;62:790–6.

Huang da W, Sherman BT, Lempicki RA. Systematic and integrative analysis of large gene lists using David bioinformatics resources. Nat Protoc 2009;4:44–57.

Hwang AS, Kechter JA, Li X, Hughes A, Severson KJ, Boudreaux B, et al. Topical Ruxolitinib in the treatment of necrobiosis lipoidica: a prospective, open-label study. J Invest Dermatol 2024.

Kalari KR, Nair AA, Bhavsar JD, O'Brien DR, Davila JI, Bockol MA, et al. MAP-RSeq: mayo analysis pipeline for RNA sequencing. BMC Bioinformatics 2014;15:224.

Li B, Tsoi LC, Swindell WR, Gudjonsson JE, Tejasvi T, Johnston A, et al. Transcriptome analysis of psoriasis in a large case-control sample: RNA-seq provides insights into disease mechanisms. J Invest Dermatol 2014;134:1828–38.

Liang Y, Tsoi LC, Xing X, Beamer MA, Swindell WR, Sarkar MK, et al. A gene network regulated by the transcription factor VGLL3 as a promoter of sex-biased autoimmune diseases. Nat Immunol 2017;18:152–60.

Love MI, Huber W, Anders S. Moderated estimation of fold change and dispersion for RNA-seq data with DESeq2. Genome Biol 2014;15:550.

Marwaha S, Knowles JW, Ashley EA. A guide for the diagnosis of rare and undiagnosed disease: beyond the exome. Genome Med 2022;14:23.

McPhie ML, Swales WC, Gooderham MJ. Improvement of granulomatous skin conditions with tofacitinib in three patients: a case report. SAGE Open Med Case Rep 2021;9:2050313X211039477.

Nguyen TM, Craig DB, Tran D, Nguyen T, Draghici S. A novel approach for predicting upstream regulators (PURE) that affect gene expression [published correction appears in Sci p. 2024;14:13291]. Sci Rep 2023;13:18571.

Nugent S, Coromilas AJ, English JC 3rd, Rosenbach M. Improvement of necrobiosis lipoidica with topical Ruxolitinib cream after prior nonresponse to compounded topical tofacitinib cream. JAAD Case Rep 2022;29:25–6.

Oprea TI, Bologa CG, Brunak S, Campbell A, Gan GN, Gaulton A, et al. Unexplored therapeutic opportunities in the human genome [published correction appears in Nat Rev Drug Discov 2018; 17:377] Nat Rev Drug Discov 2018;17:377.

Paik H, Chung AY, Park HC, Park RW, Suk K, Kim J, et al. Repurpose terbutaline sulfate for amyotrophic lateral sclerosis using electronic medical records. Sci Rep 2015;5:8580.

Perfetto L, Briganti L, Calderone A, Cerquone Perpetuini A, Iannuccelli M, Langone F, et al. Signor: a database of causal relationships between biological entities. Nucleic Acids Res 2016;44:D548–54.

Pushpakom S, Iorio F, Eyers PA, Escott KJ, Hopper S, Wells A, et al. Drug repurposing: progress, challenges and recommendations. Nat Rev Drug Discov 2019;18:41–58.

Rau A, Marot G, Jaffrézic F. Differential meta-analysis of RNA-seq data from multiple studies. BMC Bioinformatics 2014;15:91.

Rendon A, Schäkel K. Psoriasis pathogenesis and treatment. Int J Mol Sci 2019;20:1475.

Roessler HI, Knoers NVAM, van Haelst MM, van Haaften G. Drug repurposing for rare diseases. Trends Pharmacol Sci 2021;42:255–67.

Severson KJ, Costello CM, Brumfiel CM, Patel MH, Butterfield RJ, Nelson SA, et al. Clinical and morphological features of necrobiosis lipoidica. J Am Acad Dermatol 2022a;86:1133–5.

Severson KJ, Patel MH, Brumfiel CM, Breen I, Butterfield RJ, Nelson SA, et al. Comorbidities and diabetic complications in patients with necrobiosis lipoidica. J Am Acad Dermatol 2022b;86:891–4.

Sheils TK, Mathias SL, Kelleher KJ, Siramshetty VB, Nguyen DT, Bologa CG, et al. TCRD and Pharos 2021: mining the human proteome for disease biology. Nucleic Acids Res 2021;49:D1334–46.

Sirota M, Dudley JT, Kim J, Chiang AP, Morgan AA, Sweet-Cordero A, et al. Discovery and preclinical validation of drug indications using compendia of public gene expression data [published correction appears in Sci Transl Med 2011;3:102er7]. Sci Transl Med 2011;3:96ra77.

Srivastava PK, van Eyll J, Godard P, Mazzuferi M, Delahaye-Duriez A, Van Steenwinckel J, et al. A systems-level framework for drug discovery identifies Csf1R as an anti-epileptic drug target. Nat Commun 2018;9:3561.

Tsoi LC, Iyer MK, Stuart PE, Swindell WR, Gudjonsson JE, Tejasvi T, et al. Analysis of long non-coding RNAs highlights tissue-specific expression patterns and epigenetic profiles in normal and psoriatic skin. Genome Biol 2015;16:24.

Tsoi LC, Rodriguez E, Degenhardt F, Baurecht H, Wehkamp U, Volks N, et al. Atopic dermatitis is an IL-13-dominant disease with greater molecular heterogeneity compared to psoriasis. J Invest Dermatol 2019;139:1480–9.

Türei D, Korcsmáros T, Saez-Rodriguez J. OmniPath: guidelines and gateway for literature-curated signaling pathway resources. Nat Methods 2016;13:966–7.

Weth FR, Hoggarth GB, Weth AF, Paterson E, White MPJ, Tan ST, et al. Unlocking hidden potential: advancements, approaches, and obstacles in repurposing drugs for cancer therapy. Br J Cancer 2024;130:703–15.

Zador Z, King AT, Geifman N. New drug candidates for treatment of atypical meningiomas: an integrated approach using gene expression signatures for drug repurposing. PLoS One 2018;13:e0194701.